Journal of Applied Polymer Science

Performance and structure changes of the aromatic *co*-polysulfonamide fibers during thermal-oxidative aging process

Jinchao Yu,[1] Kang Chen,[1] Xiaoyun Li,[2] Feng Tian,[2] Shenghui Chen,[3] Yumei Zhang,[1] Huaping Wang[1]

[1]State Key Laboratory for Modification of Chemical Fibers and Polymer Materials, College of Materials Science and Engineering, Donghua University, Shanghai 201620, China

[2]Shanghai Institute of Applied Physics Chinese Academy of Sciences, Shanghai, 201204, China

[3]Shanghai Tanlon Fiber Co, Ltd, Shanghai 201419, China

Correspondence to: Y. Zhang (E-mail: zhangym@dhu.edu.cn)

ABSTRACT: The changes in performance during thermal-oxidative aging process of the aromatic *co*-polysulfonamide (*co*-PSA) fibers over a broad temperature range from 250 °C to 320 °C have been investigated. In addition, the mechanism of thermal-oxidative aging process has been studied by using structural information obtained from the fibers at varying length scales. The results showed that a significant reduction in tensile strength was observed compared with that of initial modulus during aging process. Macroscopically, thermal-oxidative aging mainly causes color changes of fibers and thermally induced macro defects begin to appear only at 320 °C for 100 h. On a micro level, the crystal structure of fibers remained stable and did not show significant changes expect that aging at 320 °C. In addition, thermo-degradation as well as crosslinking has been observed primarily in amorphous region. With the increase of temperature and time duration, the crosslinking became more dominant and crosslinking density increases. Correspondingly, the fibril length decreases due to degradation and then increases due to the formation of crosslinked structures within the fibers. The results suggest that molecular degradation is the main cause of strength loss and the formation of crosslinking structure within the fibers contributes to the retention of modulus and improvement of creep resistance. © 2016 Wiley Periodicals, Inc. J. Appl. Polym. Sci. **2016**, *133*, 44078.

KEYWORDS: ageing; fibers; structure-property relations; thermal properties

Received 28 February 2016; accepted 9 June 2016
DOI: 10.1002/app.44078

INTRODUCTION

Polysulfonamides (PSA) fibers exhibit excellent chemical, thermal stability, high limiting oxygen index for combustion (LOI, up to 33%), and low dielectric constants. The unique combination of properties of PSA fibers lead to their applicability in many fields including flame-retardant protection gear, high-temperature gas filtration as well as electrical insulation, and so on.[1–3] Much attention has always been attracted because of further advancements in the technology and application of *co*-polysulfonamide (*co*-PSA) fibers.

Hitherto, extensive studies have been carried out on the optimization of spinning process during the formation of PSA fibers in order to improve their performance.[4–9] In fact, the utility of fibers is also an important issue that worth full concern, because it is likely that while in use, the fibers will be exposed to their relative utility environments (e.g. either intentionally or accidentally to thermal environment), which in turn can alter their structure and performance. However, only few reports have referred to the utilization properties of PSA fibers. Usually, the usability of heat-resistant fibers was assessed mainly from the tenacity retention during or after thermal exposure. Wang[2] found that the strength retention of *co*-PSA fibers at 250 °C can attain up to 70%, even at 300 °C, it can still keep more than 50%. They also reported that the strength loss of *co*-PSA fibers is relatively small after heat-treated at 250 °C and 300 °C in air for 100 h, the strength retention can also reach over 90% and 80%, respectively. Similarly, Ren[10] pointed out that the strength of *co*-PSA fibers was not found to decrease after exposure at 200∼250 °C in air for 200 h. Yet, the structure changes induced by thermal exposure were still not fully explored which is not conducive to provide feedback constructively for the process control of spinning.

Actually, thermal exposure at selected temperatures can cause the multilayer structure of fibers change from chemical

Additional Supporting Information may be found in the online version of this article.

structure to macrostructure. For example, Jain and Vijayan[11] investigated thermal exposures caused deterioration in the initial characteristics of Nomex fibers and described the degree of aging by reduction in crystallinity, weight, and mechanical properties. They also found that surface damages of the fibers in the form of groove-like opening, minute holes, and material deposits were introduced during thermal exposure process. Hindeleh and Abdo[12] studied the thermal-oxidative aging behavior of Kevlar 49 fibers in static air at 150 °C for periods ranging between 1 and 150 days. The results showed that there is no change in crystallinity within the first 7 days. A decrease from 74.8% to 62.3% occurred in the period between 7 and 44 days, after which no further change occurred. Thermal-oxidative aging helped the microparacrystallite size to grow, but after 44 days of aging the sizes decreases slightly. Downing[13] also point out the Kevlar-29 fibers subjecting thermal exposure may occur to degrade and form free-radical within the fibers, resulting in the formation of interchain crosslinks, which is helpful to the enhancement of compressive properties. Similar phenomenon also can be observed in the polybenzoxazole (PBO).[14]

Usually, the *co*-PSA fibers can be used safely below 250 °C for a long-term time. However, in some severe conditions, the fibers has to be exposed over 250 °C, which may accelerate its degradation failure. Therefore, it is of interest to gain knowledge about the response of the *co*-PSA fibers to thermal-oxidative environments with the temperature more than 250 °C and less than its glass transition temperature ($T_g > 350$ °C). The object of this work is to evaluate the mechanical performance of *co*-PSA fibers after thermal-oxidative aging, which was conducted by tensile, creep test as well as dynamic mechanical analysis (DMA). And then the mechanism of thermal-oxidative aging was explored from structural information in different length scales, which can be characterized by dissolution, X-ray photoelectron spectroscopy (XPS), small-angle X-ray scattering (SAXS), wide-angle X-ray scattering (WAXS), and scanning electron microscope (SEM). Some useful information about a greater margin of safety in applications could be suggested.

EXPERIMENTAL

Materials

The aromatic *co*-polysulfonamide fibers (*co*-PSA) were made commercially available by Shanghai Tanlon Fiber Co., Ltd, China. The chemical structure of *co*-PSA fibers has been shown by the common formula in Scheme 1. The fibers were prepared by using wet-spinning technology and subjected to coagulation, plastic stretching, washing, drying, heat stretching, and heat setting. The final fibers were about 12 μm in diameter.

Thermal-Oxidative Aging Treatment

Unconstrained bundles of *co*-PSA fibers ~2 mm thick and ~70 mm in length were placed in muffle furnace and subjected to thermal exposures in air. The temperatures chosen were 250 °C, 280 °C, 300 °C, and 320 °C, respectively. Choice of temperatures more than its long-term working temperature (250 °C) and close to the glass transition temperature ($T_g > 350$ °C)[15] were deliberate and was intended to investigate thermal-oxidative aging performances of *co*-PSA fibers in some severe environment. Durations of cumulative exposure (t) ranged from 30 to 200 h. The choice of the exposure time was arbitrary.

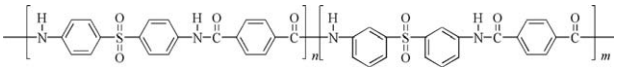

Scheme 1. Chemical structure of *co*-PSA fibers (n:m = 3:1).

Characterization

Prior to and during various stages of thermal-oxidative aging, the structure and properties of *co*-PSA fibers were characterized. Details of the experimental procedures are as follows.

The discoloration of fibers at different conditions was recorded by using digital camera. The surface morphology analysis of *co*-PSA fibers was carried out by means of a Hitachi S-3000N scanning electron microscope (SEM). The fibers were pasted on a sample-carrier, and then sputtered with gold prior to observation.

The stress–strain curves of a single fiber were recorded using a XQ-2 tensile tester with a gauge length of 20 mm and an extension rate of 20 mm/min. At least 50 samples were tested for each samples and the tenacity, elongation at break, and initial modulus were calculated averagely.

The solubility of various *co*-PSA fibers was investigated by immersing fibers into N′N-dimethylacetamide (DMAc) at 60 °C for 24 h. The resultant insoluble residue was separated from the solvent by filtration, washed, and then dried in the vacuum drier at 105 °C to constant weight. The insoluble fraction of the fibers in DMAc was determined by the insoluble mass relative to the original mass.

Creep tests were performed on a Hitachi thermal mechanical analyzer (TMA/SS 7100). The gauge length of creep test was 15 mm. The displacement of the sample was detected by linear variable differential transformer with an accuracy of 0.01 μm and analyzed by a computer. All creep experiments were conducted with applied stress of 100 MPa at a temperature of 250 °C, and at a creep duration, which was constant and equal to 120 min.

The dynamic mechanical (DMA) behavior of the *co*-PSA fibers was analyzed using TA Q800 V7.5 instrument to obtain the loss factor (tan δ). The frequency applied was 1 Hz over a temperature range from 40 °C to 400 °C at 5 °C/min in the temperature-frequency sweeping mode.

The X-ray photoelectron spectroscopic (XPS) experiments were performed on PHI5300 system with Al Kα radiation (energy hν=1,486.6 eV). The X-ray anode was run at 250 W and the high voltage was kept at 14.0 KV with a detection angle at 54°. The pass energy was fixed at 23.5, 46.95, or 93.90 eV to ensure sufficient resolution and sensitivity. The base pressure of the analyzer chamber was about 5×10^{-8} Pa. The sample was directly pressed to a self-supported disk with the size 10 × 10 mm and mounted on a sample holder then transferred into the analyzer chamber.

Synchrotron X-ray measurements were carried out at Shanghai Synchrotron Radiation Facility (SSRF) on beam line (BL16B) with an X-ray wavelength of 0.124 nm. A bundle of *co*-PSA

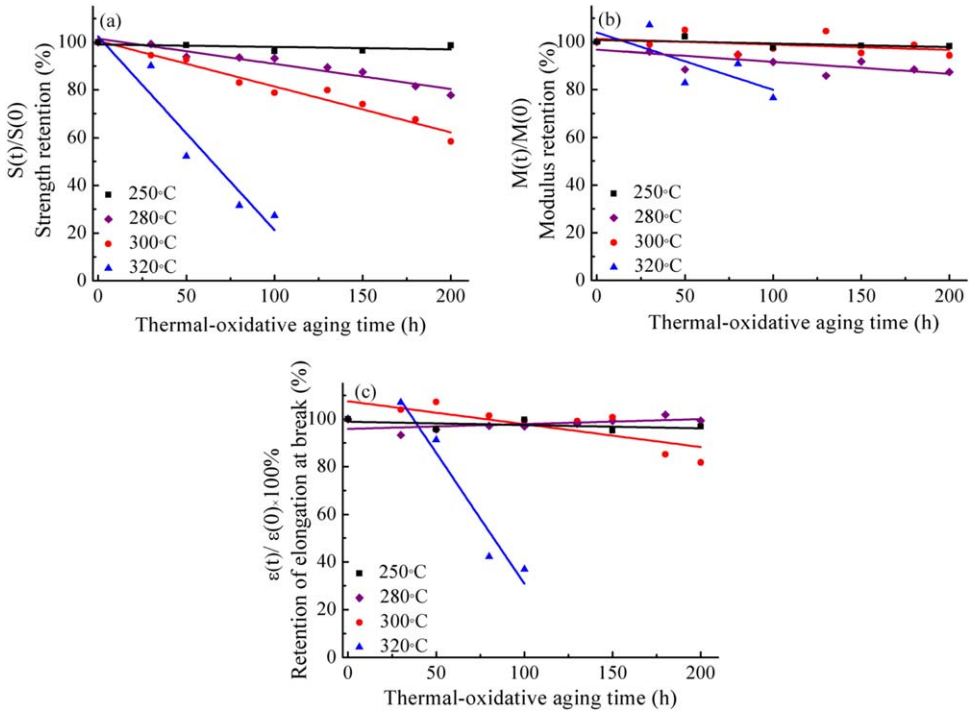

Figure 1. Retention of the tensile strength (S), tensile modulus (M), and percentage elongation at break (ε) of *co*-PSA fibers at different thermal-oxidative conditions. [Color figure can be viewed in the online issue, which is available at wileyonlinelibrary.com.]

fibers were put on a sample holder with the fiber direction perpendicular to the X-ray beam. Two types of X-ray measurements were performed respectively: WAXS and SAXS. Two-dimensional (2D) WAXS and SAXS patterns were acquired using a Mar-CCD (165) detector. The sample-to-detector distances for WAXS and SAXS were 236.49 mm and 1,790 mm, respectively. All data analysis (background correction, radial, and azimuthal integration) was carried out using the Xpolar software (Precision works NY) as reported in our previous paper.[8,16]

RESULTS AND DISCUSSION

Mechanical Properties of *co*-PSA Fibers at Different Thermal-Oxidative Aging Conditions

Usually, exposure to a thermal oxidative environment may induce the deterioration of performance or affect the durability of *co*-PSA fibers. Thus, it is important to investigate mechanical properties to determine whether the fibers remain serviceable or not after aging. Tensile tests were carried out and the retention of strength, modulus, and elongation at break were plotted in Figure 1.

It can be noticed that the mechanical performances of *co*-PSA remain about the same when thermal aged at 250 °C. As expected, when thermal-oxidative aged at higher temperature, the tensile strength of *co*-PSA fibers decreases obviously vs. aging duration. Interestingly, it does not introduce any significant reduction in tensile modulus of *co*-PSA fibers expect exposure to 320 °C. In particular, the tensile modulus of *co*-PSA fibers aging at 300 °C is even larger than that of fibers aging at 280 °C. These features suggest that exposures to 250 to 300 °C may introduce some structural changes that enable retention of the tensile modulus, which will be discussed in the following section. In addition, Figure 1(c) shows that the *co*-PSA fibers turned to be brittle obviously, because the percentage elongation at break decreased significantly with cumulative thermal exposure at 320 °C. At this stage, the surface damage of fibers and some other microstructural changes may be the main cause of deterioration of fiber performance, which will be described in the later part.

Creep Behavior of *co*-PSA Fibers at Different Thermal-Oxidative Aging Conditions

During the thermal-oxidative aging process, the chemical reactions such as degradation or crosslinking within the fibers inevitably lead to the changes in molecular weight, which may affect molecular mobility under the load. Therefore, to better explain the effect of thermal-oxidative aging on the mechanical performances of *co*-PSA fibers, creep tests were equally carried out. The creep rate (Figure 2) is determined by fitting the curves with a logarithm function as follows[17,18]: $\varepsilon(t) = A^{*}\log(t) + B$, where $\varepsilon(t)$ is the strain value in %, t is time, A and B are constants. The coefficient A is the creep rate parameter (strain per decade in time). The larger value of the parameter means the poorer creep resistance. Interestingly, when plotted as function of aging time, the evolution of the creep rate parameter A of *co*-PSA fibers at various aging temperatures appears to be different trends (seen in Figure 2). Clearly, all the aged samples have larger creep rate parameters than that of original samples, which may be related to the disorientation or degradation of molecules. However, the *co*-PSA fibers aged for different time at 250 °C maintain a relatively constant value of creep rate parameter, showing that the *co*-PSA fibers are rather stable at 250 °C. In contrast, there are two stages for the value changes of creep

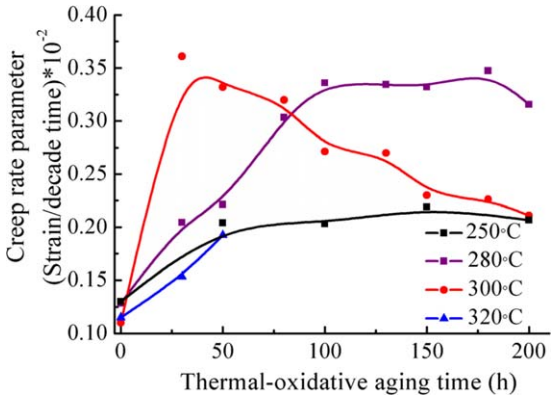

Figure 2. Variation of creep rate parameters of *co*-PSA fibers at different thermal-oxidative aging conditions. [Color figure can be viewed in the online issue, which is available at wileyonlinelibrary.com.]

rate parameter of *co*-PSA fibers aging at 280 °C, i.e., increases first (aging time less than 100 h) and then stabilize. Similarly, when aging at 300 °C was carried out, the creep rate parameter of *co*-PSA fibers decreases with the increase of aging time. This phenomenon suggests that fiber undergoes some structural changes such as crosslinking structure, which cause local resistance to reduce molecular segmental motion and consequent make the creep rate slow down or even decrease. In addition, for the samples aging at 320 °C, it can be found that the creep rate parameter of fibers increases with aging time, indicating that the molecular chains are easier to slip when applying the load on fibers. It also should be noted that after 80 h exposure to 320 °C, the fibers turned brittle and crumbled with handing. Therefore, they could not be used further for creep testing.

Dynamic Mechanical Analysis of *co*-PSA Fibers at Different Thermal-Oxidative Aging Conditions

The influences of thermal-oxidative aging on the structure changes also can be indirectly reflected by DMA analysis (Figure 3), which is used to characterize the mobility of molecules in amorphous region. To clarify, the highest test temperature of DMA is only set to 400 °C, because the samples are easy to stick to the clamp over this temperature. It is obvious that a continuous α relaxation process can be identified from 300∼400 °C, which correspond to the glass transition temperature.[19] It is clear that the peak temperature of α relaxation of *co*-PSA fibers would be changed, which depends on the aging conditions of fibers. For samples aging at 250 °C, it should be noted that all the *co*-PSA fibers displayed almost the same glass transition temperature around 360 °C and had similar dynamic thermomechanical behavior according to the tan δ–T curves. It indicated that the aging condition of 250 °C had little influence on the molecular movability in the amorphous regions of *co*-PSA fibers. When the fibers aged at 280 °C over 100 h, it can be found that the peak temperature of α relaxation of *co*-PSA fibers shifted to higher temperature. This phenomenon is more evident among the fibers aging at 300 °C and 320 °C. Correspondingly, the α transition peak area of these fibers was partly reduced, suggesting that the motion of molecular chain segments were restricted resulting from the thermal-oxidative aging. In short, the increase in the value of peak temperature of

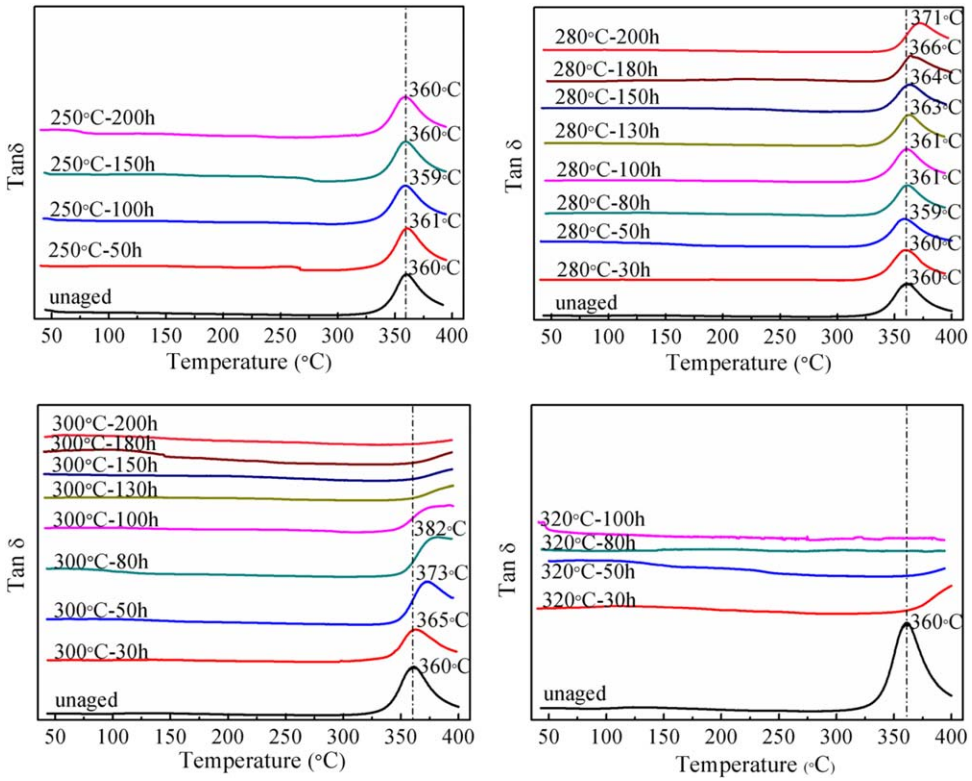

Figure 3. DMA curves of *co*-PSA fibers at different thermal-oxidative aging conditions. [Color figure can be viewed in the online issue, which is available at wileyonlinelibrary.com.]

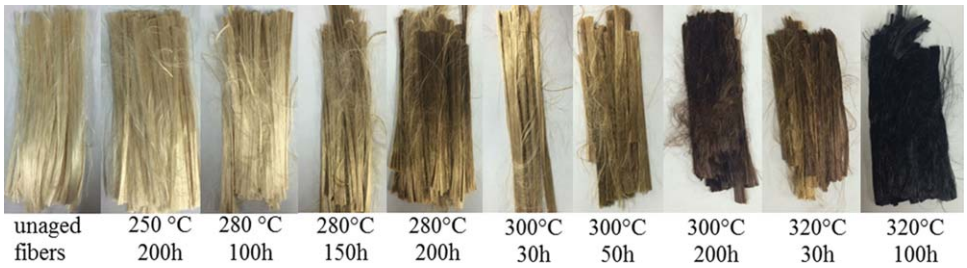

Figure 4. Photographs of *co*-PSA fibers thermal-oxidative aging at different conditions. [Color figure can be viewed in the online issue, which is available at wileyonlinelibrary.com.]

α relaxation with increasing aging time and temperature may be explained by the formation of crosslinking within the fibers, resulting in the decrease of the molecular mobility.

Appearance and Morphology Changes of *co*-PSA Fibers before and after Thermal-Oxidative Aging

It is known that the surface area of fibers will undergo more severe thermal oxidation than the interior, which may even produce some defects during this process. To confirm this, the appearance of *co*-PSA fibers thermal-oxidative aging at various temperatures and duration was investigated.

As it can be observed in Figure 4, a change of the *co*-PSA fibers from light yellow to golden brown or even to dark brown and black was noticed during thermal-oxidative aging process, which was depended on the aging temperature and time. Apparently, the color density of *co*-PSA fibers increases at lot at higher temperature and longer time. It is undoubted that this color shifting of the fibers can be ascribed to the occurrence of oxidation reactions in the aging process, which lead to the formation of an oxidized layer on the fiber surface.

Furthermore, the morphology of *co*-PSA fibers thermal-oxidative aging at different conditions presented by SEM images is summarized as shown in Figure 5 in order to illustrate damage on the surface of *co*-PSA fibers. A small number of grooves along the fibers axis are observed on the surface of unaged fibers, which is mainly formed in the coagulation stage during the wet spinning process. When exposure at 250∼300 °C, the color of *co*-PSA fibers varies greatly, but the changed in surface structure are not very noticeable, which seems to be relatively smooth. In contrast, the longitudinal surface damage such as holes formation was observed in fibers after ageing at 320 °C for 100 h. Undoubtedly, thermally induced holes or pits can be expected to lead to deterioration in the tensile properties of the *co*-PSA fibers, as shown in Figure 1.

Chemical Structure Changes of *co*-PSA Fibers before and after Thermal-Oxidative Aging

The color variations on the surface region of unaged *co*-PSA fibers imply that complex physicochemical changes take place in the chemical structure or texture. Several experiments were conducted to illustrate the changes of chemical structure with the *co*-PSA fibers. First, the dissolution test was conducted to qualitatively describe the possible reactions (degradation or crosslinking) according to the solubility of fibers after aging. If the crosslinking reaction occurred, the fibers cannot dissolve in the solvent.

As shown in Figure 6, the unaged *co*-PSA fibers can be fully dissolved in DMAc, however, the insolubility was observed in DMAc when the *co*-PSA fibers were placed in thermal-oxidative for a period of time. The cause of insoluble impurity in the dissolution process suggested that crosslinking must take place

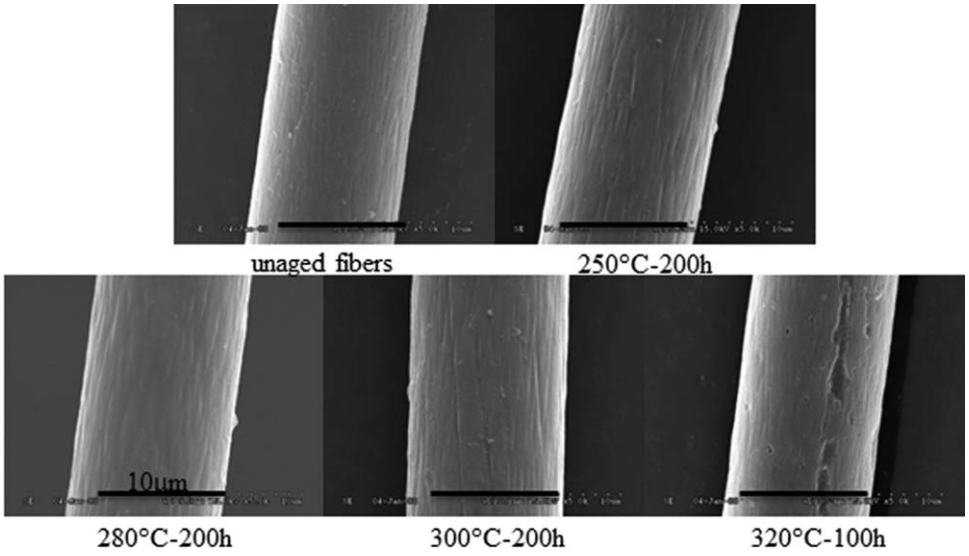

Figure 5. SEM micrographs of *co*-PSA fibers thermal-oxidative aging at different conditions.

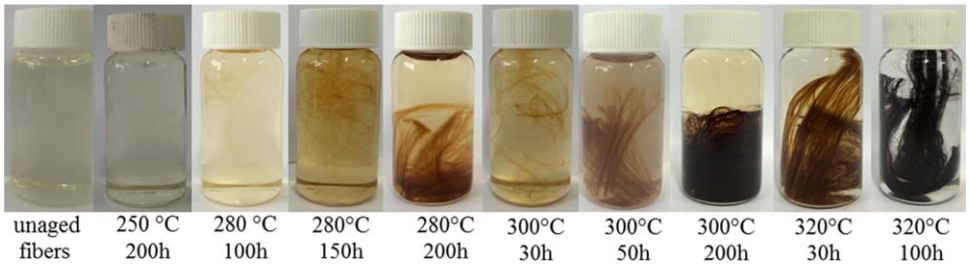

Figure 6. Dissolution photograph of *co*-PSA fibers thermal-oxidative aging at different conditions. [Color figure can be viewed in the online issue, which is available at wileyonlinelibrary.com.]

within the *co*-PSA fibers during the aging process. In fact, the insoluble fraction of the aged samples is remarkably affected by the temperature and time, i.e., higher temperature and longer time will lead to the fast increase of insolubility, indicating larger crosslinking density in fibers, as shown in Figures 6 and 7. For example, it is seen that crosslinking formation is particularly rapid above temperatures of 300∼320 °C. Similar phenomenon can also be found in other high performance fibers, such as poly(*p*-phenylene terephthalamide) (PPTA),[13] PBO,[14] and so on.

In addition, Fourier transform infrared spectroscopy (FTIR) and XPS were also used to further explain the possible changes of chemical structure of fibers after thermal-oxidative aging. Unfortunately, FTIR test failed to detect the generation of some new chemical groups due to the lower resolution and the position and intensity of adsorption peak of aged *co*-PSA fibers in FTIR spectra remains unchanged compared to the original samples (shown in the supplement Figure 1). The good news is that XPS results can reveal the surface chemical changes of the *co*-PSA fibers after the thermal-oxidative aging, as shown in Table I. It could be seen that there was a little decrease in surface-carbon, nitrogen, and sulfur concentration and increase in surface-oxygen concentration of thermal aged fibers at 320 °C for 100 h. Moreover, the ratio of oxygen to carbon atoms enhances obviously from 0.30 to 0.32 after thermal-oxidative aging for 100 h at 320 °C, while that of nitrogen to carbon atoms has no change during the thermal-oxidative aging process. These results indicate that the increase of oxygen content mainly come from the surrounding oxygen resulting in the oxidation of the sample surface during the aging processing, which may change the chemical structure of fibers to some extent.

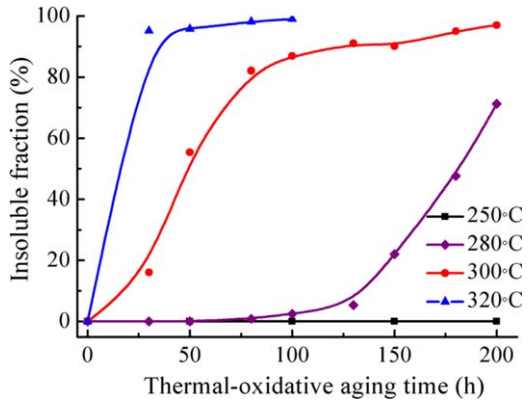

Figure 7. Insoluble fraction in DMAc of *co*-PSA fibers thermal-oxidative aging at different conditions. [Color figure can be viewed in the online issue, which is available at wileyonlinelibrary.com.]

In order to explain the changes in chemical groups before and after thermal-oxidative aging, the C_{1S} and N_{1S} spectrum was chosen and deconvolved with XPSPEAK software as shown in Figure 8. The C_{1S} spectrum before thermal-oxidative aging can be fitted with three main peaks [Figure 8(a)]. The first two peaks observed at 284.3 eV and 285.3 eV are assigned to the carbons in the aromatic rings[20]; one at 284.3 eV is ascribed to the carbon without a functional group, the other at 285.3 eV to carbon with a functional group, such as —C═O,[20,21] —N,[20,22] or —S.[22] The third peak at 287.8 eV can be attributed to the C atoms which was double-bonded to oxygen and single-bonded to nitrogen (O═C—N).[21] Also present in the Figure 8(b) was an intense N_{1S} peak with a rather symmetric shape at 399.7 eV, corresponding to the —N—C═O groups.[21] Usually, for aromatic fibers, the scission of the aromatic-NH and amide NH–CO linkages is major initial processes in the thermal degradation, which may play an importance role in the formation of amine and carboxyl free radicals then combined with oxygen to cause subsequent oxidation reactions,[23] which may lead to form the crosslinking structure. Indeed, as seen in the XPS spectrum, it exhibit the variations in its positions after thermal-oxidative aging at 320 °C for 100 h, and the main peaks from the C_{1S} and N_{1S} were shift to lower binding energy. For C_{1S} spectra of the aged fibers [Figure 8(c)], the

Table I. Relative Chemical Composition and Atomic Ratios Determined by XPS for *co*-PSA Fibers before and after Thermal-Oxidative Aging

	Chemical composition (%)				Atomic ratio	
Sample	C_{1S}	O_{1S}	N_{1S}	S_{2P}	O/C	N/C
Unaged	71.31	21.31	5.18	2.20	0.30	0.07
Aged at 320°C for 100 h	70.34	22.37	5.12	2.16	0.32	0.07

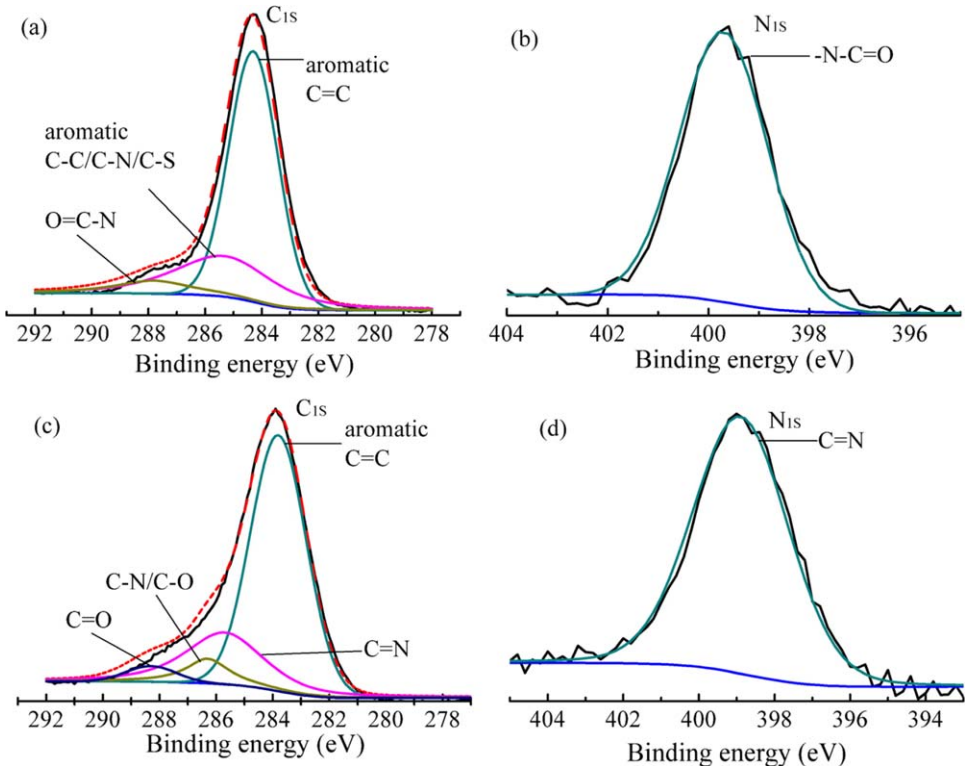

Figure 8. XPS C_{1S} (left) and N_{1S} (right) spectra of unaged (a,b) and thermal-oxidative aged (c,d) *co*-PSA fibers at 320 °C for 100 h. [Color figure can be viewed in the online issue, which is available at www.interscience.wiley.com.]

intense peak has a chemical shift of about 0.5 eV compared with the unaged one, and appears at lower binding energy, 283.8 eV, also representing to the position of aromatic carbon[24,25] or graphite C═C.[26] This can be explained on the basis of production of new free radicals and formation ring-shaped structure, which may cause the generation of crosslinking network structure-like graphite. In addition, the other peaks positioned at 285.7 eV, 286.3 eV, and 288.3 eV are assigned to C═N,[27] C─N/C─O,[28–30] and C═O,[31] respectively indicating that the molecular chains of *co*-PSA were destroyed resulting from the thermal oxidation and then generated some new groups. Also shown in Figure 8(d) are the N_{1S} spectra for the aged *co*-PSA fibers. Thermal exposure resulted in the N_{1S} peak at 399.7 eV has a shift of about 0.8 eV, corresponding to the conversion of the ─C─N to ─C═N group.[32] Honestly speaking, the chemical structure changes of *co*-PSA fibers during thermal-oxidative aging process are rather complex and this experimental result does not provide direct evidence of the reaction process. However, it does offer some indirect proof about the occurrence of crosslinking reaction.

Microstructure of *co*-PSA Fibers at Different Thermal-Oxidative Aging Conditions

The microstructure changes of *co*-PSA fibers during the thermal-oxidative aging process were also systematically investigated by WAXS and SAXS.

The crystal structural features of all *co*-PSA samples were analyzed by WAXS as shown in Figure 9. Apparently, the WAXS pattern of *co*-PSA fibers by thermal-oxidative aging for a period of 200 h at 250∼300 °C in static air changed little and the equatorial reflections, meridional reflections and the off-equatorial reflections are still visible, suggesting that the crystal structures of *co*-PSA fibers was practically unaffected. In contrast, a stronger diffuse halo was observed in the WAXS pattern when the *co*-PSA fibers subjected to thermal exposures at 320 °C for 80 h, indicating that the formation of more disorientated structure. Even worse, all the reflections had faded at 320 °C for 100 h and only a diffuse halo was observed, which means the crystal structure was destroyed and only amorphous state exist within the fibers.

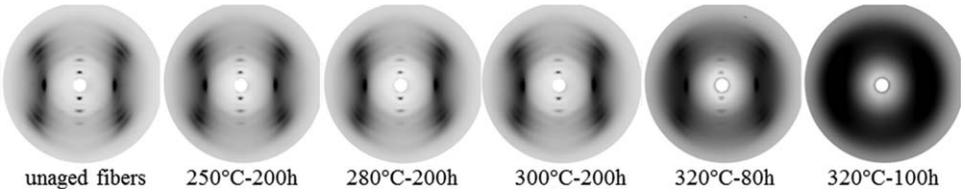

Figure 9. WAXS pattern of *co*-PSA fibers at different thermal-oxidative aging conditions.

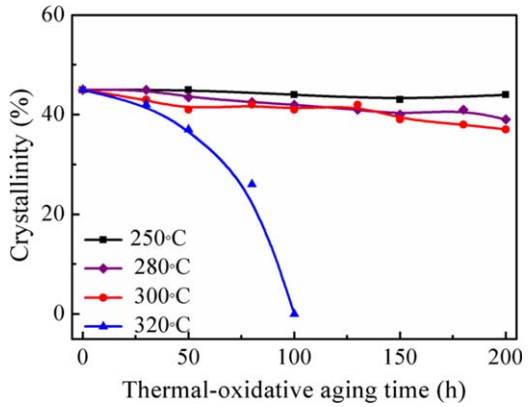

Figure 10. Variation of crystallinity of *co*-PSA fibers at different thermal-oxidative aging conditions. [Color figure can be viewed in the online issue, which is available at wileyonlinelibrary.com.]

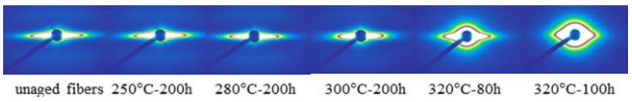

Figure 11. SAXS pattern of *co*-PSA fibers at different thermal-oxidative aging conditions. [Color figure can be viewed in the online issue, which is available at wileyonlinelibrary.com.]

To quantitatively describe the changes of crystal structure of *co*-PSA fibers during thermal-oxidative aging process, the crystallinity of fibers was calculated as shown in Figure 10. The crystallinity of the unaged fibers was found to be 45%. Thermal-oxidative aging the sample at 250 °C did not cause any change in the crystallinity. At 280 °C for 200 h, the crystallinity decreased slightly to 39%, and at 300 °C for 200 h it just dropped to 37%. The results of the crystallinity investigation suggest that the crystal structure of *co*-PSA fibers is not significantly destroyed and remains stable in the temperature region 250∼300 °C aging for 200 h. Therefore, it can be understood that at the temperature range being used, the structures changes such as disorientation, degradation or crosslinking mainly occurred in the amorphous region based on the results of creep, DMA, and solubility tests, which will be discussed later. However, when the fibers were thermally aged at 320 °C, the crystal structure of fibers damaged and the crystallinity of fibers decreased sharply over time, particularly after 100 h, the fibers are in amorphous state.

The analysis for the microstructural changes of the thermal-oxidative aging *co*-PSA fibers at large scale was done by SAXS as shown in Figure 11. According to previous studies,[8,16] the equatorial streak of small-angle diffuse scattering for heat-drawn *co*-PSA fibers is generally attributed to the presence of fibrils elongated along the fiber axis. Therefore, the average length and misorientation angle Bϕ of fibril can be determined by the method of Ruland,[33] as shown in Figure 12. It is clear that the there was no change in the fibril length when fibers aging at 250 °C. In addition, the value of fibril length began to decrease gradually at 280 °C only after 100 h. While at higher thermal-oxidative aging temperatures (300 °C and 320 °C), the value of fibril length decreased first and then increased. This decrease in fibril length can be attributed to fibril shrink or degradation. It must be said that the shrink process usually need short duration and the thermal-oxidative aging temperature is lower than the glass transition temperature of *co*-PSA fibers. In addition, any obvious changes of observed values of the diameter of *co*-PSA

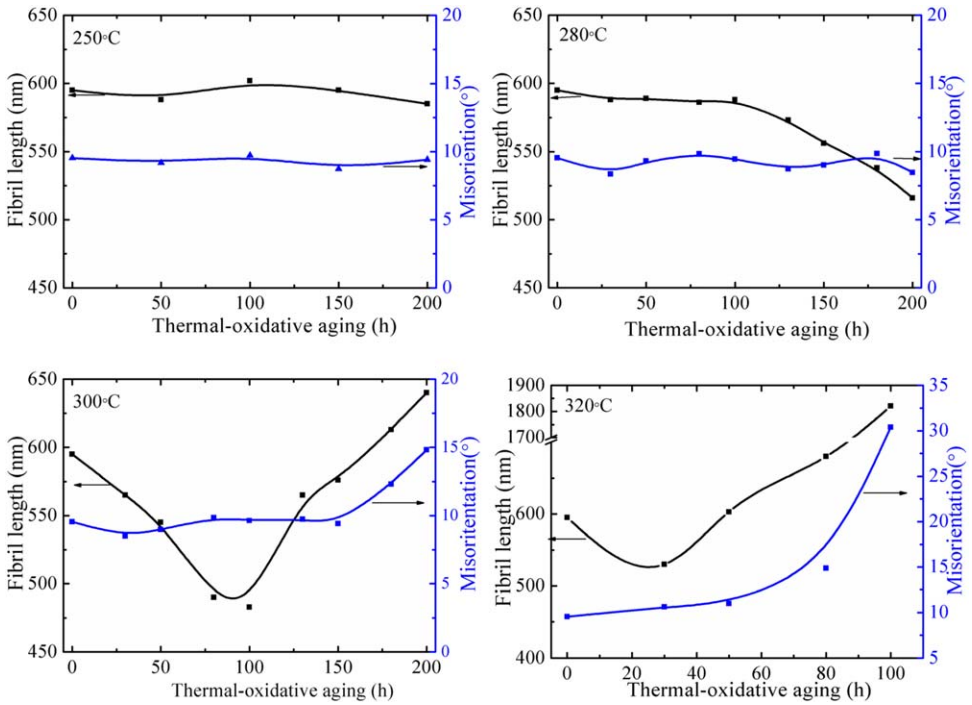

Figure 12. Variation of fibril size within *co*-PSA fibers at different thermal-oxidative aging conditions. [Color figure can be viewed in the online issue, which is available at wileyonlinelibrary.com.]

fibers with time in thermal-oxidative aging period have not been found. Therefore, it is reasonable to deduce that the decrease in fibril length during the aging process is mainly due to degradation and the effect of shrinkage is to be small or non-existent. As mentioned above, for aromatic polymers, thermal degradation may result in the production of radical and further reactions caused by free radical can lead to the formation of crosslinking. This is the reason why the fibril length increases after aging for a period. Furthermore, from Figure 12, it can be found that the fibril orientation of *co*-PSA fibers is free of discernible thermal-oxidative aging influence within the temperature range from 250 °C to 280 °C based on the value of misorientation. After 150 h at 300 °C or 50 h at 320 °C, the value of misorientation increases with time, suggesting the fibril orientation decreased, which may have adverse impact on the performance of fibers.

The Relationship between the Structure and Performances of *co*-PSA Fibers at Different Thermal-Oxidative Aging Conditions

The mechanical properties changes can be understood from the changes of *co*-PSA fibers during the thermal-oxidative aging process. From the above analysis, it should be noted that the structure of *co*-PSA fibers are stable at 250 °C, and the fiber performances were essentially unaffected by thermal exposure. As thermal-oxidative aging at 280∼320 °C, degradation and crosslinking are co-existent within fibers. At lower temperature and shorter duration, e.g. 280∼320 °C, the molecule degradation is predominant reaction with *co*-PSA fibers. Subsequently, intermolecular crosslinking is the major reaction and the crosslinking density increase with the increase of temperature and duration. At this stage, there are little significant changes in the crystalline region expect that of fibers thermal-oxidative aging at 320 °C, in this time the crystalline region was severely destroyed. The decrease in fiber strength during the thermal-oxidative aging process is caused mainly by degradation of *co*-PSA molecular chains. In contrast, the formation of crosslinking structure can restrict the movement of chains, thereby limiting modulus loss and improving the creep resistance and relaxation temperature of fibers.

CONCLUSIONS

Thermal-oxidative aging studies of *co*-PSA fibers were conducted over the temperature range of 250∼320 °C. It has been found that the *co*-PSA fibers have higher stability at 250 °C. When fibers were subjected to thermal exposure at higher temperature, it has been observed that the loss of strength caused by thermal-oxidative aging occurs more rapidly than that of initial modulus of *co*-PSA fibers. During this process, there is little damage in the crystal structure of *co*-PSA fibers expect that treated at 320 °C, while it mainly led to molecular degradation in amorphous region and the formation of crosslinked structures. The molecular degradation is the main cause of the strength loss and the crosslinked structures within the fibers, which thus contributes to the retention of modulus and improvement of creep resistance.

ACKNOWLEDGMENTS

This work was financially supported by National Natural Science Foundation of China (11079015 and 51273039), Chinese Universities Scientific Fund (CUSF-DH-D-2014024), and State Key Laboratory for Modification of Chemical Fibers and Polymer Materials, Donghua University (LK1506).

REFERENCES

1. Wang, S.; Ling, A.; Wu, L.; Gao, Y.; Liu, S.; Wang, Z.; Sheng, L.; Kang, D. *Desalination* **1987**, *62*, 221.
2. Wang, X.; Zhang, Y. *China Textile Leader* **2005**, *1*, 18. (Chinese)
3. Ban, Y.; Zhang, Y.; Ren, J. *Technical Textiles* **2006**, *12*, 33. (Chinese)
4. Banduryan, S. I.; Shchetinin, A. M.; Grechishki, A. V.; Iovkeva, M. M.; Papkov, S. P. *Fibre Chem.* **1976**, *7*, 631.
5. Sokira, A. N.; Efimova, S. G.; Shchetinin, A. M.; Frenkel', G. G.; Iovleva, M. M. *Fibre Chem.* **1979**, *10*, 545.
6. Muraveva, N. I.; Konkin, A. A. *Fibre Chem.* **1973**, *4*, 127.
7. Khudoshev, I. F.; Vorosatova, G. G.; Frenkel', G. G.; Shchetinin, A. M.; Ivanova, R. S. *Fibre Chem.* **1982**, *14*, 149.
8. Yu, J.; Wang, R.; Yang, C.; Chen, S.; Wang, H.; Zhang, Y. *Polym. Int.* **2014**, *63*, 2084.
9. Yang, X.; Yu, J.; Tian, F.; Chen, S.; Wang, F.; Zhang, Y. *Rsc Adv.* **2015**, *5*, 27163.
10. Ren, J.; Wang, J.; Yu, Z. *Melliand China* **2007**, *35*, 27. (Chinese)
11. Jain, A.; Vijayan, K. B. *Mater. Sci.* **2002**, *25*, 341.
12. Hindeleh, A. M.; Abdo, S. M. *Polymer* **1989**, *30*, 218.
13. Downing, J. W.; Newell, J. A. *J. Appl. Polym. Sci.* **2004**, *91*, 417.
14. Isayeva, V. A.; Gur'yanova, V. V.; Chernikhov, A. Y.; Korshak, V. V.; Noskova, M. P.; Kotov, Y. I.; Kovarskaya, B. M. *Polym. Sci. U.S.S.R.* **1980**, *22*, 2107.
15. Ding, X.; Chen, Y.; Chen, S.; Li, J.; Wang, X.; Wang, H.; Zhang, Y. *J. Macromol. Sci.* **2012**, *51*, 1199.
16. Yu, J.; Tian, F.; Chen, S.; Wang, X.; Zhang, Y.; Wang, H. *J. Appl. Polym. Sci.* **2015**, *132*, 42343.
17. Lechat, C.; Bunsell, A. R.; Davies, P. *J. Mater. Sci.* **2011**, *46*, 528.
18. Ericksen, R. H. *Polymer* **1985**, *26*, 733.
19. Kuznetsov, G. A.; Nikiforov, N. I.; Lebedev, V. P.; Zhuravlev, V. G.; Savinov, V. M. *Polym. Sci. U.S.S.R.* **1974**, *16*, 3156.
20. Chen, W.; Zhang, J.; Fang, Q.; Hu, K.; Boyd, I. W. *Thin Solid Films* **2004**, *453*, 3.
21. Xie, Y.; Sherwood, P. M. A. *Chem. Mater.* **1992**, *5*, 1012.
22. Mark, S.; Andrey, T.; Nottbohm, C. T.; Beyer, A.; Solak, H. H.; Hinze, P.; Weimann, T.; Gölzhäuser, A. *Small* **2009**, *5*, 2651.
23. Brown, J. R.; Hodgeman, D. K. C. *Polymer* **1982**, *23*, 365.
24. Andreoli, E.; Barron, A. R. *Energ. Fuel* **2015**, *29*, 4479.

25. Majeed, R. M. A. A.; Datar, A.; Bhoraskar, S. V.; Bhoraskar, V. N. *Nucl. Instrum. Meth. B* **2007**, *258*, 345.
26. Yang, S.; Gong, Y.; Zhang, J.; Zhan, L.; Ma, L.; Fang, Z.; Vajtai, R.; Wang, X.; Ajayan, P. M. *Adv. Mater.* **2013**, *25*, 2452.
27. Zocco, A.; Perrone, A.; Broitman, E.; Czigany, Z.; Hltman, L.; Anderle, M.; Laidani, N. *Diam. Relat. Mater.* **2002**, *11*, 98.
28. Liu, B.; Pei, X.; Wang, Q.; Sun, X.; Wang, T. *Surf. Interface Anal.* **2012**, *44*, 372.
29. Ektessabi, A. M.; Hakamata, S. *Thin Solid Films* **2000**, *377*, 621.
30. Štěpánková, M.; Šašková, J.; Grégr, J.; Wiener, J. *Chem. Listy* **2008**, *102*, 1515.
31. Inagaki, N.; Tasaka, S.; Ohmori, H.; Mibu, S. *J. Adhes. Sci. Technol.* **1996**, *10*, 243.
32. Yegen, E.; Lippitz, A.; Treu, D.; Unger, W. E. S. *Surf. Interface Anal.* **2008**, *40*, 176.
33. Ruland, W. *J. Polym. Sci. C* **1969**, *28*, 143.